# Chapter 2

# Vaidya-Tikekar Model: Exact Solutions

## 2.1 Introduction

The exterior of a static, spherically symmetric distribution of matter is uniquely described by the Schwarzschild metric:

$$ds^2 = -\left(1-\frac{2M}{r}\right)dt^2 + \left(1-\frac{2M}{r}\right)^{-1}dr^2 + r^2\left(d\theta^2 + Sin^2\theta d\phi^2\right), \qquad (2.1)$$

where, $M$ is the mass of the distribution observed by a distant observer. The interior solutions of static perfect fluid spheres, however, are not unique and consequently the problem has been taken up by many authors, e.g., [92] & [93]. There are several techniques to construct models for spherically symmetric objects, e.g., Fodor [94] has prescribed a new algorithm to generate solutions for spherical perfect fluid distribution of matter. Recently, Finch and Skea [95] and Delgaty and Lake [96] have reviewed a large class of interior solutions and pointed out various aspects of those solutions. The large abundance of exact solutions to Einstein's field equations for a static, spherically symmetric perfect fluid star allows us to look for solutions capable of describing realistic stars.

To obtain an exact solution to the Einstein's field equations for a static spherically symmetric perfect fluid configuration, we write the interior metric as (in geometrised units with $8\pi G = c = 1$)

$$ds^2 = -e^{2\gamma(r)}dt^2 + e^{2\mu(r)}dr^2 + r^2(d\theta^2 + \sin^2\theta d\phi^2) \tag{2.2}$$

in standard coordinates $x^i = (t, r, \theta, \phi)$. The quantities $\gamma(r)$ and $\mu(r)$ are the gravitational potentials.

As we consider spherically symmetric objects only, we must have

$$G_{\theta\theta} = G_{\phi\phi}, \tag{2.3}$$

where, $G_{\mu\nu}$ is the Einstein tensor. In addition, we impose the pressure isotropy condition

$$G_{rr} = G_{\theta\theta} = G_{\phi\phi}. \tag{2.4}$$

The perfect fluid spherically symmetric configuration, may, in that case represent a star under certain regularity conditions ( [97]), viz.: (1) isotropy of pressure, (2) regularity of the geometry at the origin, (3) positive definiteness of the energy density and pressure at the origin, (4) vanishing of the pressure at some finite radius, (5) monotonic decrease of pressure and energy density with increasing radius, and (6) subluminal speed of sound; although the necessity of condition (6) is arguable in the case of very compact stars [97]. Nevertheless, very few solutions obey these regularity conditions and at the same time represent a realistic situation. We have found a new class of solutions which satisfy all these conditions and is found to be very useful in describing a class of compact stellar objects. Here we mention some of the solutions obeying all these criteria and pick up the general solution given by Mukherjee *et al* [67] which will be used extensively by us in the chapters to follow.

## 2.2 Equilibrium configuration of a star: Standard approach

The equilibrium structure of a self-gravitating object is derived from the equations of hydrostatic equilibrium. The standard procedure for studying a self-gravitating, static, spherical star is to make use of the Tolman [98], Oppenheimer and Volkoff [3] equations (TOV) given by

$$\frac{dp}{dr} = -(\rho+p)\frac{2M(r)+pr^3}{r^2(1-\frac{2M(r)}{r})} \tag{2.5}$$

$$\frac{dM(r)}{dr} = \frac{1}{2}\rho r^2. \tag{2.6}$$

Here $\rho$ represents the energy density and $p$ is the isotropic pressure, expressed in geometrized units of $length^{-2}$. If the equation of state (EOS) $p = p(\rho)$ is known, all the properties of the star can be determined. One integrates the TOV equations numerically, using the boundary conditions (i) $M(0) = 0$, (ii) $p(0) = p(\rho_c)$, (iii) $p(b) = 0$ and (iv) $e^{2\gamma(b)} = 1 - \frac{2M}{b}$, where $b$ is the radius and $M = M(b)$ is the total mass of the star as measured gravitationally from outside. For a particular EOS and a chosen parameter (e.g., central density) there is one and only one stellar configuration with a particular mass and radius.

The problem is that there are many physical situations in which one simply does not know the equation of state either because of uncertainties in the basic physics (e.g. the physics of matter above nuclear matter density in neutron stars), or in the case of a very compact star where deconfinement is a possibility, it may not be a good suggestion to use a single EOS to describe the entire star. An alternative approach has to be explored in such situations.

## 2.3 Alternative method

In situations where the equation of state (EOS) of superdense compact objects is uncertain or unknown, it will be useful to follow an alternative approach. One starts here with an ansatz for one of the metric functions and integrate the pressure isotropy condition to determine the other. The solution then characterises a class of static spherically symmetric perfect fluid configuration and provides the relevant EOS. The approach was first considerted by Vaidya and Tikeker [63] who prescribed an ansatz for the geometry for the $t = constant$ hypersurface. The 3-surface has a simple geometrical interpretation. If embedded in a 4-Euclidean space

$$d\sigma^2 = dx^2 + dy^2 + dz^2 + du^2, \tag{2.7}$$

a spheroidal 3-surface is defined by

$$\frac{x^2 + y^2 + z^2}{R^2} + \frac{u^2}{k^2} = 1. \tag{2.8}$$

If we write

$$x = RSin\delta Cos\theta Cos\phi,$$
$$y = RSin\delta Sin\theta Sin\phi,$$
$$z = RSin\delta Cos\theta,$$
$$u = kCos\delta,$$

equation (2.8) becomes,

$$d\sigma^2 = (R^2Cos^2\delta + k^2Sin^2\delta)d\delta^2 + R^2Sin^2\delta(d\theta^2 + Sin^2\theta d\phi^2). \tag{2.9}$$

Again writing, $r = RSin\delta$, we get

$$d\sigma^2 = \frac{1 + \lambda\frac{r^2}{R^2}}{1 - \frac{r^2}{R^2}}dr^2 + r^2(d\theta^2 + Sin^2\theta d\phi^2) \tag{2.10}$$

where we substituted, $\lambda = \frac{k^2}{R^2} - 1$. This 3-surface is spherically symmetric and well behaved for $r < R$ and $\lambda > -1$. For $\lambda = -1$, the hypersurface is flat and $\lambda = 0$ gives spherical space.

The line element for a general static spherically symmetric configuration has the standard form given in (2.2). Capitalizing on the above observation we may now assume the $g_{rr}$ metric component in (2.2) as

$$e^{2\mu} = \frac{1 + \lambda r^2/R^2}{1 - r^2/R^2}. \tag{2.11}$$

The the geometry of the configuration, thus obtained, is governed by the parameters $R$ and $\lambda$.

We assume that the space-time region, thus obtained, is filled with a perfect fluid and the energy-momentum tensor for such a fluid has the form

$$T_{ij} = (\rho + p)u_i u_j + p g_{ij} \tag{2.12}$$

where $u^i$ is the 4-velocity of the fluid. Due to spherical symmetry $u^i$ may be chosen as: $u^i = (e^{-\gamma}, 0, 0, 0)$.

The Einstein field equations $G_{ij} = R_{ij} - \frac{1}{2}g_{ij}R = T_{ij}$, for the metric (2.2), then, reduce to

$$\rho = \frac{(1 - e^{-2\mu})}{r^2} + \frac{2\mu' e^{-2\mu}}{r} \tag{2.13}$$

$$p = \frac{2\gamma' e^{-2\mu}}{r} - \frac{(1 - e^{-2\mu})}{r^2} \tag{2.14}$$

$$p = e^{-2\mu}\left(\gamma'' + \gamma'^2 - \gamma'\mu' + \frac{\gamma'}{r} - \frac{\mu'}{r}\right) \tag{2.15}$$

where primes denote differentiation with respect to $r$.

Equations (2.14) and (2.15) may be combined to give

$$\gamma'' + \gamma'^2 - \gamma'\mu' - \frac{\gamma'}{r} - \frac{\mu'}{r} - \frac{(1 - e^{2\mu})}{r^2} = 0. \tag{2.16}$$

Equation (2.16) results from the pressure isotropy condition. To find the solution to equation (2.16), one has to make some ad hoc assumptions for $\gamma$ or $\mu$. Assuming

the form of $\mu$ as in (2.11), we introduce the transformation

$$\begin{aligned} \psi &= e^{\gamma} \\ x^2 &= 1 - \frac{r^2}{R^2} \end{aligned}$$

so that (2.16) can be written as

$$\left(1 + \lambda - \lambda x^2\right) \psi_{xx} + \lambda x \psi_x + \lambda \left(\lambda + 1\right) \psi = 0. \tag{2.17}$$

Here the suffix $x$ represents differentiation with respect to $x$. This equation has been comprehensively studied by a number of authors. We give here a few solutions of equation (2.17) which have utilized the ansatz of Vaidya and Tikekar [63]. These solutions may represent a toy model for a class of superdense stars.

### 2.3.1 The solution of Vaidya and Tikekar [63]

For a particular choice of the curvature parameter $\lambda = 2$, Vaidya and Tikekar [63] obtained an exact solution of equation (2.17), and the line element obtained by them has the form

$$ds^2 = -\left[Ax\left(1 - \frac{4x^2}{9}\right) + B\left(1 - \frac{2x^2}{3}\right)^{3/2}\right]^2 dt^2 + \frac{3 - 2x^2}{x^2} dr^2 + r^2 d\Omega^2. \tag{2.18}$$

where, $A$ and $B$ are constants. $(d\Omega^2 = d\theta^2 + Sin^2\theta d\phi^2)$.

### 2.3.2 The solution of Tikekar [64]

Tikekar [64] obtained an exact solution of equation (2.17) for $\lambda = 7$ and the line element in this case has the form

$$ds^2 = -\left[C(1 - \frac{7x^2}{2} + \frac{49x^4}{24}) + Dx(1 - \frac{7x^2}{8})^{3/2}\right]^2 dt^2 + \frac{8 - 7x^2}{x^2} dr^2 + r^2 d\Omega^2 \tag{2.19}$$

where, $C$ and $D$ are constants.

### 2.3.3 The solution of Maharaj & Leach [66]

Maharaj & Leach [66] obtained two catagories of polynomial solutions of equation (2.17) for discrete values of the parameter $\lambda$. For $\lambda = (2n-1)^2 - 2$, the solutions are given by:

$$e^{\gamma} = \psi = A\sum_{i=0}^{n} \frac{(n+i-2)!}{(n-i)!(2i)!}(-l)^i x^{2i} + B(1+\lambda-\lambda x^2)^{3/2} \sum_{i=0}^{n-2} \frac{(n+i)!}{(n-i-2)!(2i+1)!}(-l)^i x^{2i+1} \tag{2.20}$$

while for $\lambda = 4n^2 - 2$, the solutions are:

$$\psi = A\sum_{i=0}^{n} \frac{(n+i-1)!}{(n-i)!(2i+1)!}(-m)^i x^{2i+1} + B(1+\lambda-\lambda x^2)^{3/2} \sum_{i=0}^{n-1} \frac{(n+i)!}{(n-i-1)!(2i)!}(-m)^i x^{2i}, \tag{2.21}$$

with,

$$l = 4 - \frac{1}{n(n-1)},$$

$$m = 4 - \frac{4}{4n^2-1}$$

and $n = 2, 3$ etc.

### 2.3.4 The solution of Mukherjee *et al* [67]

The general solution of equation (2.17) for any value of $\lambda$ was obtained by Mukherjee *et al* [67]. As we shall use this solution extensively in the chapters to follow, we discuss here various features of this solution.

We straight way start with the equation (2.17). To obtain the general solution, a new variable is defined

$$z = \left(\frac{\lambda}{\lambda+1}\right)^{1/2} x. \tag{2.22}$$

The equation (2.17) then gets the form

$$(1-z^2)\psi_{zz}(z) + z\psi_z(z) + (\lambda+1)\psi(z) = 0 \tag{2.23}$$

where the subscript $z$ denotes differentiation with respect to $z$.

The solution to this equation for an integer $n$, where, $n = (\lambda+2)^{1/2}$, can be written as

$$\psi = A_1 T_{n+1}^{-3/2}(z) + A_2(1-z^2)^{3/2} T_{n-2}^{3/2}(z), \tag{2.24}$$

where $T_\alpha^\beta$ is a Gegenbauer function [99] and $A_1$ & $A_2$ are constants.

Differentiating equation (2.24) with respect to $z$ we get,

$$\psi_z = A_1 T_n^{-1/2}(z) + A_2(n+1)(n+3)(1-z^2)^{1/2} T_{n-1}^{1/2}(z). \tag{2.25}$$

We note that $nT_n^{-1/2}(z)$ and $(1-z^2)^{1/2}T_{n-1}^{1/2}(z)$ are actually Tschebyscheff polynomials. For an integer $n$ and real $z$ with $0 < z \leq [\lambda/(\lambda+1)]^{1/2}$, these polynomials can be expressed in terms of trigonometric functions:

$$nT_n^{-1/2}(z) = (2/\pi)^{1/2} \cos(n \cos^{-1} z), \tag{2.26}$$

$$(1-z^2)^{1/2} T_{n-1}^{1/2}(z) = (2/\pi)^{1/2} \sin(n \cos^{-1} z). \tag{2.27}$$

Substituting these values in equation (2.25) and integrating we obtain $\psi$ in terms of trigonometric functions as

$$\psi(z) = e^\gamma = A\left[\frac{\cos[(n+1)\zeta+\delta]}{n+1} - \frac{\cos[(n-1)\zeta+\delta]}{n-1}\right], \tag{2.28}$$

where $\zeta = \cos^{-1} z$, and $A$ and $\delta$ are constants. Although the solution (2.28) is obtained by considering initially integral values of $n$, it can now be continued analytically for any real $\lambda > -2$. Thus we get the general solution for any $\lambda > -2$. Physical considerations may, however, put further constraints on the value of $\lambda$.

### General features of the solution:

In this model, energy-density $\rho$ and pressure $p$ are given, respectively, by

$$\rho = \frac{1}{R^2(1-z^2)}\left[1 + \frac{2}{(\lambda+1)(1-z^2)}\right] \tag{2.29}$$

$$p = -\frac{1}{R^2(1-z^2)}\left[1 + \frac{2z\psi_z}{(\lambda+1)\psi}\right]. \tag{2.30}$$

The radius of the star, $b$, is determined by the condition that pressure should vanish at the boundary, i.e., $p = 0$ at $r = b$. From (2.30), this gives

$$z_b \frac{\psi_z(z_b)}{\psi(z_b)} = -\frac{1}{2}(1+\lambda) \tag{2.31}$$

where $z_b = [\lambda/(\lambda+1)]^{1/2}(1 - b^2/R^2)^{1/2}$.

The mass contained inside a radius $r$ is given by

$$M(r) = \frac{1}{2}\int_0^r r'^2 \rho(r')dr' \tag{2.32}$$

which on integration upto $r = b$ yields

$$M(b) = \frac{(1+\lambda)b^3/R^2}{2(1+\lambda b^2/R^2)}. \tag{2.33}$$

From (2.29) and (2.30) we note that $\rho$ is obviously positive for $\lambda > -1$, while $p \geq 0$ requires $z\psi_z/\psi \leq -\frac{1}{2}(\lambda+1)$.

For $p$ to remain finite $\psi$ should not have a zero in the range $z_b \leq z \leq z_0$, where $z_0 = [\lambda/(\lambda+1)]^{1/2}$. We also require that both $d\rho/dz$ and $dp/dz$ should increase monotonically as $z$ increases from $z_b$ to $z_0$. In Fig.2.1 $p$ is plotted against $\rho$ which clearly shows that there is no singular behaviour for $p$ in the prescribed range.

This model has 4 parameters $R$, $\lambda$, $A$ and $\delta$, of which three, say, $R$, $A$ and $\delta$, can be determined by the matching conditions: (1) at $r = b$, $p = 0$ and (2) continuity of two metric coefficients across the boundary. The choice of the remaining parameter $\lambda$, then, fixes the equation of state. Thus while in the standard approach, the inputs are the central density and the equation of state, in the present model $b$ and $\lambda$ play similar roles.

Note that $r < R$ corresponds to $b > 2M$ as in the case of the Schwarzschild interior solution. Further the black hole event horizon in the present case can be approached either by letting $r \longrightarrow R$ or $\lambda \longrightarrow \infty$.

To determine the velocity of sound, we differentiate equation (2.28) which gives,

$$u = \frac{\psi_z}{\psi} = \frac{(n^2-1)\Big[\sin[(n-1)\zeta+\delta] - \sin[(n+1)\zeta+\delta]\Big]}{\sqrt{1-z^2}\Big[(n+1)\cos[(n-1)\zeta+\delta] - (n-1)\cos[(n+1)\zeta+\delta]\Big]}. \tag{2.34}$$

From equations (2.29) and (2.30) we get,

$$\frac{dp}{d\rho} = \frac{z(1-z^2)^2u^2 - (1-z^2)u}{z(1-z^2)(1+\lambda)+4z}, \tag{2.35}$$

where, $u$ is defined in equation (2.34). The velocity of sound is defined by $v_s = \sqrt{\frac{dp}{d\rho}}$.

The most stringent constraint in a stellar model comes if we require that the sound propagation be causal; i.e. $\frac{dp}{d\rho} < 1$. This implies

$$\frac{1}{(1-z^2)}\Big(\frac{1}{2z} - D\Big) \leq \frac{\psi_z}{\psi} \leq \frac{1}{(1-z^2)}\Big(\frac{1}{2z} + D\Big), \tag{2.36}$$

where

$$D = [4 + 1/4z^2 + (1+\lambda)(1-z^2)]^{1/2}. \tag{2.37}$$

Again, $p \geq 0$ gives

$$\frac{\psi_z}{\psi} \leq -\frac{\lambda+1}{2z} \quad . \tag{2.38}$$

Combining the two constraints, we get the effective bound

$$\frac{1}{1-z^2}\Big(\frac{1}{2z} - D\Big) \leq \frac{\psi_z}{\psi} \leq -\frac{\lambda+1}{2z}, \tag{2.39}$$

for a realistic model. Eqn. (2.39) readily leads to a lower bound

$$\lambda > \frac{3}{17}. \tag{2.40}$$

This clearly excludes the flat space ($\lambda = -1$).

In Fig.2.1, the slope of the $p$ versus $\rho$ curve is always less than that of $\rho = p$, which shows that $dp/d\rho < 1$ always. Further it lies below and never intersects the $\rho = 3p$ curve indicating $\rho > 3p$ and hence satisfying the strong energy condition.

The constraint (2.39) leads to an upper bound on possible values of $\overline{b} = b/R$, which reads as

$$(1-\overline{b}^2) \geq \frac{\lambda^2 + 5\lambda + 12 - (17\lambda^2 + 82\lambda + 129)^{1/2}}{\lambda(5+\lambda)}. \tag{2.41}$$

In Fig.2.2, the upper bound on $\overline{b}$ is plotted against $\log_{10}\lambda$. The figure shows that for a given $\overline{b}$, there correspond two values of $\lambda$.

Equations (2.33) and (2.41) also lead to an upper bound on $M/b$, which measures the compactness of the star. The upper bound approaches the Schwarzschild limit 1/2 asymptotically as $\lambda$ tends to infinity. The upper bound on $M/b$ increases monotonically from 0 to $\frac{1}{2}$ as $\lambda$ is increased from its lowest value $\frac{3}{17}$ as shown in Fig.2.3. This shows that for a given radius $b$, stars with larger $\lambda$ will be more compact.

From equation (2.29) we get the central density of the star

$$\rho_c = 3(\lambda + 1)/R^2, \tag{2.42}$$

from which the parameter $R$ can also be determined. In Table 2.1, values of various parameters in this model for different choices of the parameter $\lambda$ are given. The mass and radius chosen in this case are $M = 0.88\ M_\odot$ and $b = 7.7\ km$, respectively.

We may sum up by observing that

- $p$ is well-behaved in the prescribed range for $z$. The curve $p$ versus $\rho$ indicates the implicit equation of state for the fluid.
- $dp/d\rho < 1$ always as slope of the solid curve is less than that of $\rho = p$ curve.
- both $\rho > p$ and $\rho > 3p$ (the weak and strong energy conditions) are satisfied as can be seen by comparing with the other two curves in Fig.2.1.

Thus all the physical conditions are satisfied.

## 2.4 Discussions

To conclude, we have noted that the general soution given by Mukherjee *et al* [67] describes a class of static spherically symmetric distribution of matter in hydrostatic equilibrium, satisfying all physical constraints. Also, as the solution is in simple trigonometric form, the model can be handled easily. Various applications of this model will be taken up in the chapters to follow.

| $\lambda$ | $R(km)$ | $\delta$ | $A$ | $\left(\frac{dp}{d\rho}\right)_{r=0}$ | $\left(\frac{dp}{d\rho}\right)_{r=b}$ |
|---|---|---|---|---|---|
| 2 | 20.224 | 2.23367 | 0.9332 | 0.3418 | 0.3518 |
| 5 | 27.545 | 2.41532 | 1.6913 | 0.2714 | 0.2847 |
| 10 | 36.627 | 2.49738 | 2.9926 | 0.2479 | 0.2624 |
| 20 | 50.073 | 2.5449 | 5.61083 | 0.2361 | 0.2511 |
| 50 | 77.488 | 2.57512 | 13.4818 | 0.2291 | 0.2446 |
| 100 | 108.779 | 2.58577 | 26.6039 | 0.2268 | 0.2424 |
| 200 | 153.264 | 2.59118 | 52.8501 | 0.2256 | 0.2413 |

Table 2.1: Values of various parameter of the model for different choices of the parameter $\lambda$ for a star of mass $M = 0.88\ M_{\odot}$ & radius $b = 7.7\ km$.

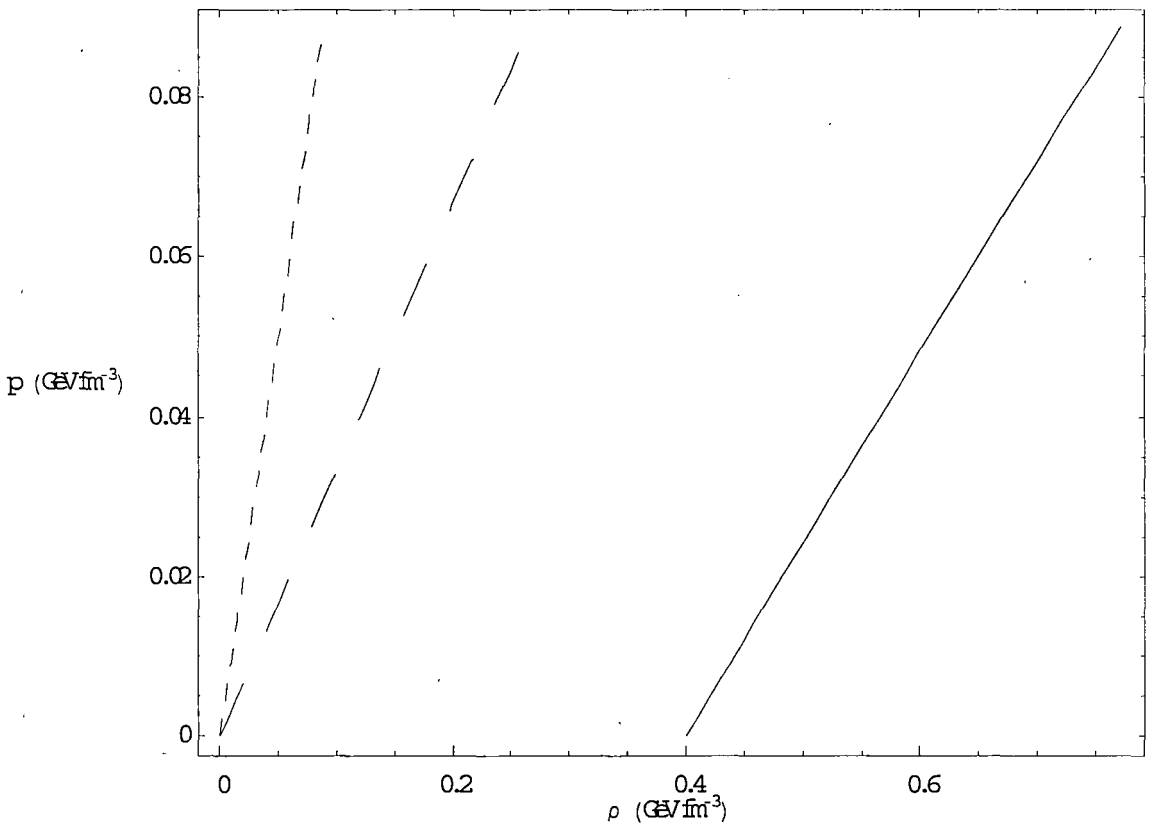


Figure 2.1: Equation of state of a star of mass $M = 0.88\ M_{\odot}$ and radius $b = 7.7\ km$ (solid line), while short and long dashed lines represent $\rho = p$ and $\rho = 3p$ curves, respectively. Here, $\lambda = 100$, $\delta = 2.58577$ and $R = 108.779\ km$.

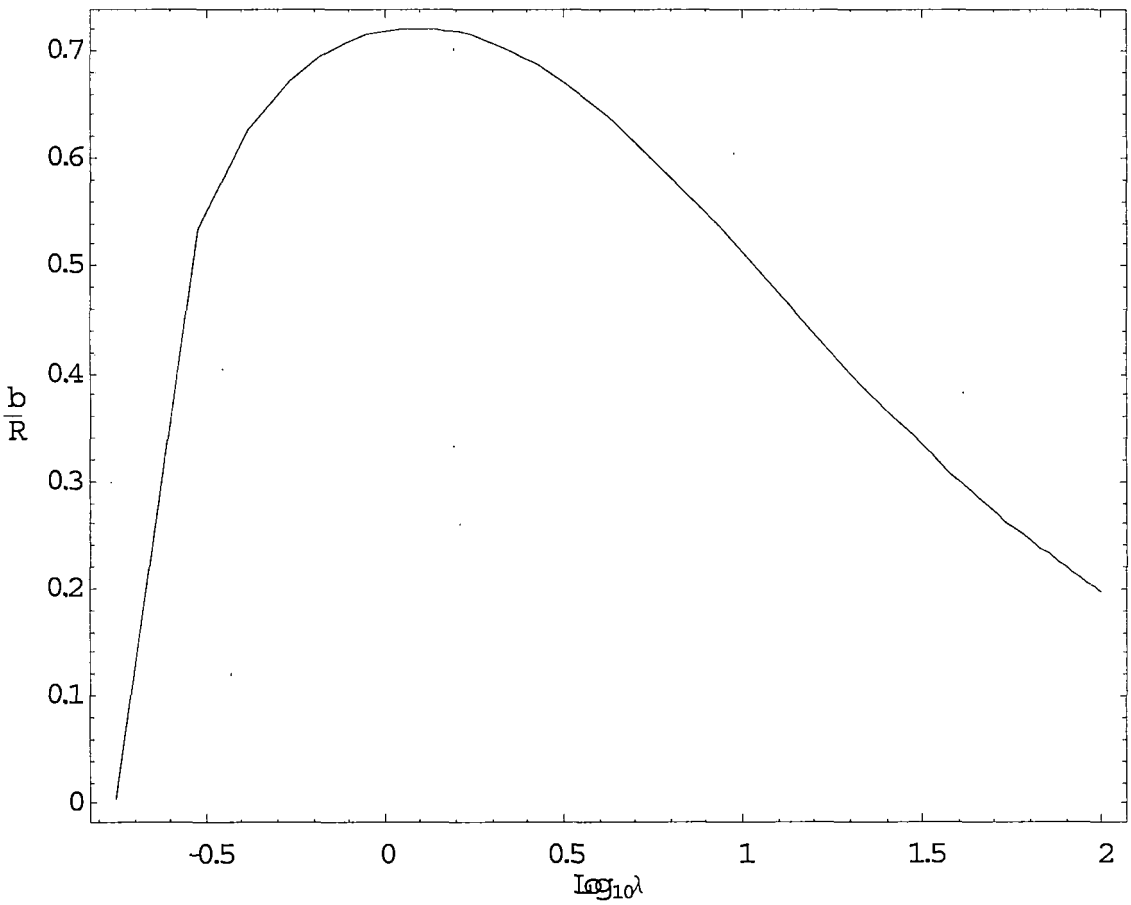


Figure 2.2: Upper bound on the possible values of $\frac{b}{R}$ plotted agained $Log_{10}\lambda$.

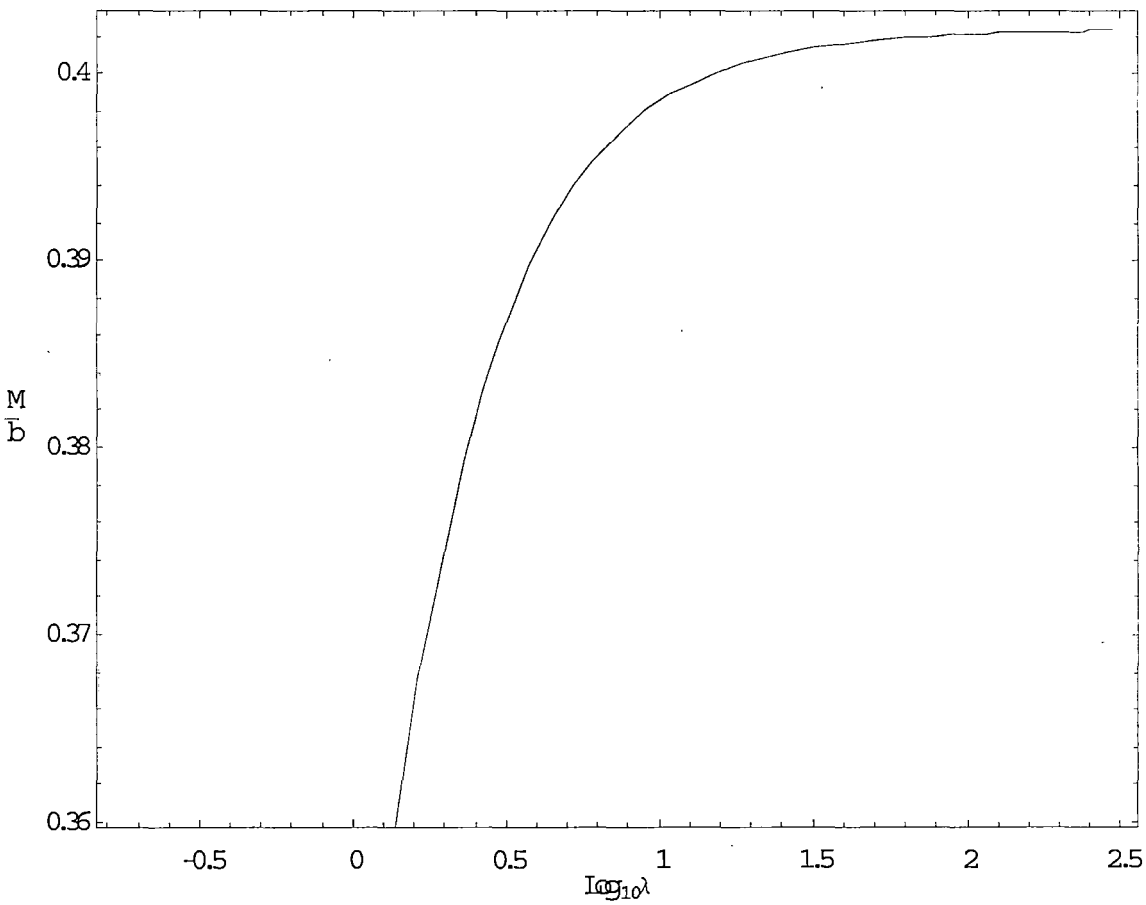


Figure 2.3: Upper bound on the possible values of $\frac{M}{b}$ plotted agained $Log_{10}\lambda$.